Published in final edited form as:
ACS Chem Biol. 2016 June 17; 11(6): 1552–1560. doi:10.1021/acschembio.6b00083.

Highly dynamic interactions maintain kinetic stability of the ClpXP protease during the ATP-fueled mechanical cycle

Alvaro J. Amor[#1], **Karl R. Schmitz**[#1], **Jason K. Sello**[2], **Tania A. Baker**[1,3], and **Robert T. Sauer**[1,*]

[1]Department of Biology, Massachusetts Institute of Technology, Cambridge, MA 02139

[2]Department of Chemistry, Brown University, Providence, RI 02912

[3]Howard Hughes Medical Institute, Massachusetts Institute of Technology, Cambridge, MA 02139

[#] These authors contributed equally to this work.

Abstract

The ClpXP protease assembles in a reaction in which an ATP-bound ring hexamer of ClpX binds to one or both heptameric rings of the ClpP peptidase. Contacts between ClpX IGF-loops and clefts on a ClpP ring stabilize the complex. How ClpXP stability is maintained during the ATP-hydrolysis cycle that powers mechanical unfolding and translocation of protein substrates is poorly understood. Here, we use a real-time kinetic assay to monitor the effects of nucleotides on the assembly and disassembly of ClpXP. When ATP is present, complexes containing single-chain ClpX assemble via an intermediate and remain intact until transferred into buffers containing ADP or no nucleotide. ATP binding to high-affinity subunits of the ClpX hexamer prevents rapid dissociation but additional subunits must be occupied to promote assembly. Small-molecule acyldepsipeptides, which compete with the IGF loops of ClpX for ClpP-cleft binding, cause exceptionally rapid dissociation of otherwise stable ClpXP complexes, suggesting that the IGF-loop interactions with ClpP must be highly dynamic. Our results indicate that the ClpX hexamer spends almost no time in an ATP-free state during the ATPase cycle, allowing highly processive degradation of protein substrates.

Abstract

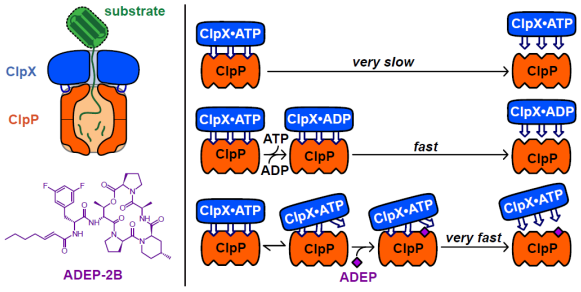

[*]corresponding author: bobsauer@mit.edu.

The ATP-powered ClpXP protease consists of the AAA+ ClpX hexamer and the ClpP peptidase, which contains two heptameric rings.[1] ClpX can bind one or both heptameric faces of ClpP, recognizes specific protein substrates via ssrA tags or other peptide degrons, and uses the energy of ATP hydrolysis to unfold and translocate substrates through an axial channel and into the degradation chamber of ClpP (Figure 1a). ClpX binding to ClpP requires ATP or ATPγS, a slowly hydrolyzed ATP analog, but is not observed in the absence of nucleotide or in the presence of ADP.[2–5] However, the role of ATP in stabilizing ClpXP complexes is poorly characterized. Moreover, the kinetics of ClpXP assembly and disassembly have not been carefully studied, in part because established binding assays rely on changes in ClpX or ClpP activity, require the continual presence of ATP/ATPγS, and/or are poorly suited for measuring rapid changes in assembly state.

ClpX hexamers dissociate at low concentrations, an event that is also nucleotide dependent,[2] potentially complicating studies of ClpP binding. However, ClpX subunits lacking the N domain ($ClpX^{\Delta N}$) can be linked using genetically encoded tethers, and single-chain $ClpX^{\Delta N}$ pseudohexamers retain wild-type levels of mechanical activity, as shown by their ability to collaborate with ClpP in degradation of ssrA-tagged substrates.[6] Pseudohexamer variants have been used to assess the number of active subunits needed for function, to show that mechanical activity requires subunit switching from ATP-binding to non-binding conformations, to establish that pore loops cooperatively grip substrates, to determine subunit-specific ATP affinities, and to visualize single-molecule unfolding and translocation in optical-trapping experiments.[6–15]

Most stabilization of ClpXP complexes arises from contacts between hydrophobic clefts on the periphery of the heptameric ClpP ring and flexible loops in the ClpX hexamer that contain an IGF or related tripeptide sequence (Figure 1a,b).[5,16–18] Contacts between axial pore-2 loops in ClpX and stem-loop structures in ClpP also contribute to ClpXP stability,[16] but elimination of these axial interactions impairs binding less than deletion of a single IGF loop from the ClpX hexamer.[16] Interestingly, small-molecule acyldepsipeptides, such as ADEP-2B, also bind to the ClpP clefts, mimicking IGF-loop binding (Figure 1c).[19–21] ADEPs have antibacterial activity because they open the axial ClpP pore, causing indiscriminate degradation of unstructured proteins.[22–23]

Fiber-optic biosensors and bio-layer interferometry (BLI) can be used for real-time assays of macromolecular interactions, as the signal is sensitive to changes in mass on the biosensor surface.[24] Here, we use this method to examine how nucleotides and ADEPs affect the kinetics of ClpP binding to single-chain ClpX pseudohexamers, eliminating potential complications caused by hexamer dissociation. Our results show that the ATP requirements for assembly and maintenance of complex stability differ, suggest that IGF-loop interactions with ClpP are highly dynamic under conditions where the complex is extremely stable, and support a model in which the ClpX hexamer spends very little time in an ATP-free state, facilitating highly processive protein degradation.

RESULTS AND DISCUSSION

Assembly requires ATP binding

We used BLI to probe binding of an *Escherichia coli* ClpP variant to a ClpX pseudohexamer immobilized on a streptavidin-coated biosensor. The pseudohexamer consisted of *E. coli* $ClpX^{\Delta N}$ subunits covalently connected by six-residue peptide tethers with a biotin near the C-terminus ($^{sc6}ClpX^{\Delta N}$-bio; Figure 1d). Single-chain $ClpX^{\Delta N}$ supports ClpP-dependent degradation of ssrA-tagged protein substrates in solution and when immobilized to a streptavidin surface.[6,7,10–15,25,26] In a typical BLI experiment, the biosensor was sequentially loaded with $^{sc6}ClpX^{\Delta N}$-bio, transferred into ATP, moved into ATP and ClpP to allow binding, and finally transferred into ClpP-free buffer with ATP to allow dissociation (Figure 2a). In this experiment, ClpP binding to $^{sc6}ClpX^{\Delta N}$-bio saturated after ~30 s, but no dissociation was observed over several minutes. ClpP bound to $^{sc6}ClpX^{\Delta N}$-bio with similar kinetics in the presence of ATP or ATPγS (Figure 2b). Because ClpX hydrolyzes ATP ~20-times faster than ATPγS,[4] binding of these nucleotides rather than their hydrolysis rates must determine the ClpXP assembly rate. ClpP did not bind $^{sc6}ClpX^{\Delta N}$-bio in the presence of ADP or without nucleotide (Figure 2b).

We performed association experiments using ATP and different ClpP concentrations. Binding trajectories at low ClpP concentrations fit well to a single exponential, as expected for a pseudo first-order reaction, whereas a double exponential was needed to fit trajectories for ClpP concentrations ≥ 500 nM (see Figure 2c for examples). For ClpP concentrations ≤ 200 nM, the rate constants (k_{obs}) from single-exponential fits varied linearly with ClpP concentration (Figure 2d), with a slope that corresponds to the association rate constant ($6.6 \cdot 10^5$ $M^{-1}s^{-1}$). The two rate constants from the double-exponential fits varied in a hyperbolic fashion between 0.5 and 20 μM ClpP (Figure 2e), suggesting that a unimolecular reaction becomes rate-limiting in ClpXP assembly at high ClpP concentrations. The shift from single- to double-exponential assembly kinetics at high ClpP concentrations is consistent with a model in which ClpX species with different ClpP-binding properties interconvert.

We measured binding of 200 nM ClpP to $^{sc6}ClpX^{\Delta N}$-bio at different ATP concentrations, determined k_{obs}, plotted normalized values against [ATP], and fit these data to the Hill equation (Figure 3a). Assembly proceeded at half the maximal rate at an ATP concentration of ~100 μM with a Hill constant (n) of 2.1. The steady-state rate of ATP hydrolysis in the absence of ClpP was half-maximal at an ATP concentration of 42 μM (V_{max} = 73 min^{-1} enz^{-1}; n = 2.4). Thus, ~2-fold higher ATP is required for half-maximal association than for half-maximal hydrolysis (Figure 3a). This result could mean that an additional molecule of ATP must bind to a hydrolytically active ClpX hexamer to promote ClpP binding. Alternatively, ClpP-binding and non-binding subpopulations of ClpX hexamers may equilibrate, with the binding conformation having slightly weaker affinity for ATP. This model seems less likely, as K_M for ATP hydrolysis by $^{sc6}ClpX^{\Delta N}$-bio in the presence of excess ClpP was 29 μM (V_{max} = 41 min^{-1} enz^{-1}; n = 2.2), in agreement with studies showing that ClpP reduces K_M for wild-type ClpX.[4]

We measured k_{obs} values for association of 200 nM ClpP in different concentrations of ATP and ADP that totaled 2 mM (Figure 3b). As the ADP concentration increased and ATP concentration decreased, the association rate slowed appreciably. For example, 0.5 mM ATP plus 1.5 mM ADP supported ClpXP binding, but at a rate ~25-fold slower than observed with 2 mM ATP. This decrease in the association rate in the presence of excess ADP probably reflects reduced ATP binding, as a result of competitive inhibition, and increased ADP occupancy of ClpX subunits.[8]

Nucleotide dependence of dissociation

To test if ClpXP complexes require the continued presence of nucleotide, we bound ClpP to immobilized $^{sc6}ClpX^{\Delta N}$-bio in the presence of ATP and transferred the biosensor into ClpP-free buffer containing ADP, ATP, or ATPγS. ClpXP complexes dissociated with a half-life of ~5 s in the presence of ADP but remained stable in ATP or ATPγS (Figure 4a). GFP-ssrA, a good protein substrate, did not prevent rapid dissociation when ClpXP was transferred from ATP into ADP (not shown). For complexes formed with ATPγS, the half-life after transfer into ClpP-free buffer containing ADP was ~20 s, (Figure 4b). As ClpX hydrolyzes ATP more rapidly than ATPγS,[4] loss of ATP through faster hydrolysis appears to result in faster ClpP dissociation. Indeed, after transfer into nucleotide-free buffer, ATP-stabilized ClpXP dissociated ~50-times faster than ATPγS-stabilized ClpXP or an ATP-stabilized ClpXP complex containing ATPase-defective REEREE ClpX (Figure 4c). The REEREE complex dissociated with similar kinetics in buffers containing no nucleotide or ADP (not shown). By contrast, ATPγS-stabilized ClpXP was more stable in nucleotide-free buffer (Figure 4c) than in buffer containing ADP (Figure 4b), suggesting that ADP binding to unoccupied ClpX subunits stimulates ATPγS hydrolysis or release.

These results show that ClpX-bound ATP or ATPγS that leaves by dissociation or hydrolysis must be replaced to maintain stable ClpXP complexes. When we transferred ATP-stabilized complexes into ClpP-free buffer with different concentrations of ATP, rapid dissociation was only observed at ATP concentrations of 10 μM or less (Figure 4d). As half-maximal assembly required 20-fold higher ATP concentrations, occupancy of a subset of high-affinity ClpX sites appears to be sufficient to maintain a kinetically stable complex. This result is consistent with experiments that show that different subunits in the ClpX hexamer bind ATP with a range of affinities.[8] ClpXP complexes transferred into buffer with a 7:1 mixture of ADP:ATP (2 mM total) were ~100-fold more kinetically stable than those transferred into ADP alone (Figure 4e), suggesting that complexes containing a mixture of ADP-bound and ATP-bound ClpX subunits are quite stable.

In ClpP-free buffer containing 2 mM ATP, little dissociation of ClpXP complexes was observed over 1000 s when the biosensor was washed twice with fresh buffer, moved into buffer containing non-biotinylated $^{sc6}ClpX^{\Delta N}$ to prevent rebinding of dissociated ClpP, or transferred into buffer containing the GFP-ssrA substrate (Figure 4f). Substantially longer BLI experiments were not possible because of sample evaporation. Assuming that fewer than 5% of ClpXP complexes dissociate in 15 min, the upper limit for the dissociation rate constant is ~$6 \cdot 10^{-5}$ s^{-1}. Based on this value and an association rate constant of $6.6 \cdot 10^5$ $M^{-1}s^{-1}$, an affinity of ~100 pM or tighter would be predicted for ClpP binding

to $^{sc6}ClpX^{\Delta N}$-bio. We were unable to obtain reliable equilibrium response values at sub-nM ClpP concentrations. A hyperbolic fit of the equilibrium BLI response versus total ClpP from 1–20 nM predicted half-maximal binding at ~160 ± 75 pM (Figure 4g), although the absence of data below 80% binding make the fit unreliable. Moreover, the fitted half-maximal value is an upper bound because the amount of $^{sc6}ClpX^{\Delta N}$-bio bound to the biosensor and thus the free ClpP concentration at half-maximal binding are unknown.

ADEP-induced dissociation

ADEPs bind to the same ClpP clefts as the IGF loops of ClpX.[19–21] Notably, even in the presence of ATP, addition of 50 μM ADEP-2B caused extremely rapid dissociation of ClpXP complexes (Figure 5a), ruling out a strictly competitive model in which ADEPs simply prevent ClpX rebinding following spontaneous dissociation. Instead, ADEP-2B must bind to the ClpXP complex and actively promote ClpX dissociation, possibly by a mechanism that involves transient unbinding of an IGF loop from a ClpP cleft and filling of this cleft by ADEP. ADEP-induced dissociation (~1 s half-life) was faster than ADP-induced dissociation (~5 s half-life), and 200 nM ADEP-2B promoted similar rates of dissociation for ATP-stabilized and ATPγS-stabilized ClpXP complexes (Figure 5b), indicating that ATP hydrolysis is not required for ADEP-induced dissociation effect.

ClpXP dissociation rates determined at different ADEP-2B concentrations fit well (R^2 = 0.994) to a hyperbolic equation expected if binding of just one ADEP-2B molecule to an appropriate ClpP site causes ClpX dissociation (Figure 5c). By contrast, mechanisms requiring binding of two or three ADEP-2Bs to identical and independent ClpP sites predict sigmoidal curves that fit more poorly (see Figure 5c legend). Strikingly, ~50 μM ADEP-2B was required for 50% stimulation of ClpXP dissociation (Figure 5c), whereas ~200 nM ADEP-2B resulted in 50% stimulation of decapeptide cleavage by ClpP alone or 50% inhibition of ClpXP assembly (Figure 5d). As discussed below, these results support a dynamic-competition model for ADEP-induced dissociation.

Stepwise assembly

Our results show that the ClpXP assembly rate increases linearly with low concentrations of ClpP, as expected for a bimolecular reaction,. However, this rate saturates at high ClpP concentrations, supporting a model in which the rate-limiting step switches from a bimolecular to a unimolecular reaction. For example, single-chain ClpX could initially collide with ClpP to form an unstable intermediate in which only one or a few IGF loops in the ClpX hexamer interact with ClpP, with docking of the remaining loops becoming the rate-limiting unimolecular step in formation of the stable complex at high ClpP concentrations. Following assembly, however, ClpXP complexes are extremely stable in buffers containing ATP, unless ADEPs are also present. It is possible that these aspects of assembly and disassembly might not apply to unlinked ClpXP complexes or be observed using assays other than BLI. For example, unlinked ClpXP might be less kinetically stable because of ClpX hexamer dissociation, or association might be strictly second-order if ClpX was not surface bound.

Dynamic IGF-cleft interactions

ADEP, a small-molecule antibiotic, binds in the same ClpP clefts as the IGF loops of ClpX, and ADEP or ClpX binding opens the axial pore of ClpP.[17,19–21,27] Based on these observations, we anticipated that ADEPs would be competitive inhibitors of ClpX binding to ClpP. However, a strictly competitive model requires dissociation of ClpXP complexes before ADEPs can bind and prevent reassociation. By contrast, we find that high ADEP-2B concentrations reduce the ClpXP half-life to ~1 s, accelerating dissociation by more than 10^4-fold. Moreover, the concentration dependence of ADEP-2B-induced ClpXP dissociation suggests that binding of a single ADEP to the ClpXP complex is sufficient to drive dissociation. In principle, ADEP binding to an empty cleft on the ClpP ring might drive an allosteric conformational change that results in ClpXP dissociation (Figure 6a). However, based on differences in affinity, the free energy of ClpP binding by our single-chain ClpX hexamer is far more favorable than ADEP-2B binding.[28] Thus, it is unlikely that one ADEP-binding event would be thermodynamically capable of driving the ClpXP complex into a conformation that forces rapid ClpX dissociation.

Our results support a “dynamic competition” model in which one ClpX IGF loop transiently unbinds a ClpP cleft, allowing an ADEP to bind and accelerate dissociation by preventing rebinding of the undocked loop (Figure 6b). By this model, ADEP binding to ClpP clefts that are not needed for IGF binding would not promote ClpXP disassembly and thus be “invisible” in terms of the concentration dependence of dissociation. Deletion of a single IGF loop from the ClpX hexamer impairs ClpP binding modestly.[16] Moreover, in a hexamer with six loops, steric clashes between a transiently unbound loop and a bound ADEP could dramatically destabilize the complex. In the ClpXP complex, the ADEP-binding sites that could drive ClpX dissociation would normally be inaccessible because they are occupied by IGF loops. Thus, compared to open clefts, high ADEP concentrations would be required to bind these transiently unoccupied sites. Consistently, half-maximal ADEP-2B concentrations required to accelerate ClpXP dissociation were ~250-fold higher than those required to inhibit assembly or stimulate ClpP-pore opening. Isolated IGF peptides bind weakly to ClpP,[27] and thus transient unbinding of an IGF loop in the complex should have a low energy barrier. Despite the dynamic nature of these interactions, tight overall binding presumably arises because the six contacts are mutually stabilizing and the high effective concentration of IGF loops with respect to ClpP clefts favors rebinding of any undocked loop as a consequence of the small entropic cost.

Additional mechanistic implications

IGF-loop flexibility was initially proposed to allow ClpXP docking despite the symmetry mismatch between six loops in the ClpX hexamer and seven clefts in a ClpP ring.[17] Consistent with some flexibility, the IGF loops are proteolytically accessible in free ClpX and disordered in crystal structures of ClpX ring hexamers.[7,18,29] If these loops are truly flexible, however, then why is ATP or ATPγS required for detectable binding of ClpX to ClpP? ATP binding might stabilize an IGF-loop conformation that allows it to dock efficiently with ClpP (Figure 6c). Alternatively, ATP binding might affect the geometry with which the six IGF loops are arranged with respect to the clefts on the ClpP ring (Figure 6d),

with only some IGF loops in ADP-bound or nucleotide-free ClpX able to engage ClpP clefts.

Although each subunit of ClpX has the same sequence, conformational changes create an asymmetric hexamer consisting of some subunits that cannot bind nucleotide and others that bind ATP/ADP with a range of affinities.[7,8,29,30] We find that half-maximal activation of ClpP binding by $^{sc6}ClpX^{\Delta N}$-bio requires higher ATP concentrations than half-maximal activation of ATP hydrolysis, making it likely that more ClpX subunits need to be ATP bound for ClpP binding than for ATP hydrolysis. However, concentrations of ATP that support less than 5% of the maximal ATP-hydrolysis activity can maintain substantial kinetic stability of preformed ClpXP complexes, indicating that occupancy of just high-affinity ClpX subunits suffices for this activity. ClpX hexamers containing a mixture of ATP-bound and ADP-bound subunits also bind ClpP with substantial kinetic stability relative to the rate of ATP hydrolysis.

ClpX does not hydrolyze ATP using a concerted or strictly sequential mechanism,[6] but optical-trapping experiments suggest that kinetic bursts of ATP hydrolysis in multiple subunits power substrate translocation.[12,13] One model to explain these bursts posits that all bound ATP is hydrolyzed rapidly with subsequent fast release of P_i and ADP, followed by slow rebinding of ATP.[12] This model predicts that ClpX would frequently be nucleotide-free or have only ADP-bound subunits. Our results allow estimation of an upper limit for the fraction of time that ClpXP spends in a nucleotide-free or ADP-bound state (f) during the normal ATPase cycle. Specifically, the ClpP dissociation rate constant in the absence of nucleotide or presence of ADP (< 0.07 s^{-1}) multiplied by f must be less than the dissociation rate constant in the presence of ATP (< 0.00006 s^{-1}). Thus, f must be less than 0.0008. Hence, under the conditions of our experiments, ClpXP appears to spend a very small fraction of time in an all ADP-bound or nucleotide-free state. ClpX hydrolyzes ATP at a rate of ~(1 s^{-1})•[ClpX] at ATP concentrations of 10^{-3} M or higher. If ClpX passed through a nucleotide-free state during each ATPase cycle, then the rate of ATP binding (k_a•[ATP][nucleotide-free ClpX]) would be less than (0.01 s^{-1})•[ClpX] based on a k_a value of $1.3 \cdot 10^4$ $M^{-1}s^{-1}$,[4] an ATP concentration of 10^{-3} M, and a nucleotide-free ClpX concentration of [f•ClpX]. Because the steady-state rate of ATP hydrolysis cannot be 100-fold faster than the rate of ATP binding, we conclude that a nucleotide-free state cannot be an obligatory or even common intermediate in the ATPase cycle. As a consequence, we propose that at least one subunit in the ClpX hexamer remains ATP-bound during the normal ATPase cycle, with the remaining subunits being ATP-bound, ADP-bound, or nucleotide-free depending on progress through the cycle. This mechanism would preserve ClpP binding and maintain grip on the polypeptide substrate, which is also ATP dependent.[31]

The degron of a protein substrate is degraded soon after it enters the proteolytic chamber of ClpP. If ClpXP dissociated after this event, then the remaining substrate would be released. However, with a few notable exceptions, degradation by ClpXP is highly processive even though hundreds of ATP-hydrolysis events can be required to degrade a single protein substrate.[9,32–34] This degree of high processivity is likely to occur because ClpXP complexes rarely dissociate, as they spend almost no time in an ATP-free state.

AAA+ proteolytic machines

The proteolytic complexes of other AAA+ proteases – including ClpAP, ClpCP, HslUV, Cdc48•20S, PAN•20S, Mpa•20S, and the 26S proteasome – are also stabilized in an ATP-dependent fashion by contacts between peripheral peptide or loop elements from each subunit of a AAA+ unfolding ring and clefts or grooves on the corresponding self-compartmentalized peptidase ring.[35] Except for HslUV, the assembly of all of these machines also involve a symmetry mismatch between a hexameric AAA+ unfolding ring and a heptameric protease ring. The functional significance of these mismatches is unknown and may simply represent random evolutionary solutions that worked. All AAA+ proteolytic machines must cycle through a variety of nucleotide-dependent conformations as they mechanically unfold and translocate protein substrates. As a consequence, we suspect that the interactions that stabilize these proteolytic machines will also be highly dynamic and influence their mechanisms of assembly and disassembly. Consistently, assembly chaperones for the 26S proteasomal base, which includes the $Rpt_{1–6}$ AAA+ ring, can drive its dissociation from the 20S peptidase.[36]

METHODS

Proteins

The $^{sc6}ClpX^{\Delta N}$-bio pseudohexamer was expressed from plasmid pACYC and contained an N-terminal FLAG tag (MADYKDDDDKHM); six *E. coli* $ClpX^{\Delta N}$ subunits (with C169S and K408E substitutions) connected by the sequences GGGTSG, GGTSSG, GGSSSG, GGSAGS, and GGGSSG, respectively; an AAAGLNDIFEAQKIEWH biotin acceptor peptide;[37] and a TEV-H_6 tag (ENLYFQSHHHHHH) at the C-terminus. As judged by the fraction of purified protein that bound to streptavidin, ~50% of the ClpX pseudohexamer was biotinylated *in vivo*. To prevent ATP hydrolysis, the REEREE $^{sc6}ClpX^{\Delta N}$-bio variant contained the R270K sensor-II mutation in subunits 1 and 4 and the E185Q Walker-B mutation in subunits 2, 3, 5, and 6.[5,6,30] *E. coli* ClpP was expressed from pET-22b (EMD Millipore), contained the C91V and C113A substitutions, and had a TEV-His_6 tag at the C-terminus. Both $^{sc6}ClpX^{\Delta N}$-bio and ClpP were purified from *E. coli* ER2566 cells (New England Biolabs) transformed with plasmids containing the appropriate gene under T7-promoter control. Cells were initially grown to an OD_{600} of ~0.7 at 37 °C in media containing 13 g L^{-1} peptone, 7.5 g L^{-1} yeast extract, and 5 g L^{-1} NaCl. At this time, 1 mM isopropyl β-D-1-thiogalactopyranoside (Teknova) was added and growth was continued for 4 h at room temperature. Harvested cells were resuspended in lysis buffer (20 mM HEPES, pH 7.5, 400 mM NaCl, 100 mM KCl, 20 mM imidazole, and 10% glycerol (v/v)), lysed by sonication, centrifuged at 12,000 rpm in a Sorvall SA-600 rotor, and the supernatant was incubated with Ni-NTA agarose beads (Thermo Fisher Scientific) for 1 h. The beads were transferred to a gravity column, washed with 5 volumes of lysis buffer, and $^{sc6}ClpX^{\Delta N}$-bio or ClpP protein was eluted with five 1-mL aliquots of lysis buffer plus 300 mM imidazole. Fractions containing protein were pooled and desalted into column buffer (25 mM HEPES, pH 7.5, 50 mM KCl, 10% glycerol) using a PD-10 column (GE Healthcare). Both proteins were further purified by MonoQ ion-exchange chromatography and Superdex-200 gel-filtration chromatography (GE Healthcare) as described.[16] Prior to Mono-Q, the H_6 tag on the ClpP-TEV-H_6 construct was removed by digestion with TEV protease, followed by

passage through Ni-NTA agarose to remove any H_6-tagged protein. Superdex-200 fractions containing purified $^{sc6}ClpX^{\Delta N}$-bio or ClpP were pooled and stored frozen at −80 °C. $^{sc6}ClpX^{\Delta N}$-bio concentrations were calculated for the pseudohexamer; ClpP concentrations were calculated in heptamer equivalents, the unit that binds a ClpX hexamer.

Assays

Assays were performed at 30 °C in a buffer containing 25 mM HEPES (pH 7.5), 100 mM KCl, 10 mM $MgCl_2$, 10% glycerol, 0.05% TWEEN-20 (EMD Millipore), supplemented as necessary with ATP (Sigma-Aldrich), ATPγS (Roche), or ADP (Sigma-Aldrich). ADEP-2B was synthesized as described,[28] and experiments using it contained 5% (v/v) dimethylsulfoxide (Alfa Aesar), which decreased the ClpXP association rate ~3-fold. BLI experiments were performed using an Octet RED96 instrument (ForteBio), 96-well plates (Greiner), and a sampling rate of 5 Hz. For most binding and kinetic experiments, $^{sc6}ClpX^{\Delta N}$-bio (20 nM) was loaded onto streptavidin biosensors to a BLI response of ~0.5 nm in the absence of nucleotide. In control experiments, the kinetics of ClpP binding were the same whether ATP was added after or simultaneously with $^{sc6}ClpX^{\Delta N}$-bio loading. For each set of experiments, a control sensor with bound $^{sc6}ClpX^{\Delta N}$-bio, under otherwise identical conditions, was transferred into buffer with no ClpP to determine the baseline and drift. Rates of ATP hydrolysis by $^{sc6}ClpX^{\Delta N}$-bio (200 nM) without or with ClpP (1 μM) were determined at different concentrations of ATP using a coupled assay.[38]

Data analysis

Kinetic trajectories were fit to single- or double-exponential functions using non-linear-least-squares algorithms implemented in Prism (GraphPad Software) or KaleidaGraph (Synergy Software). Trajectories were initially fit to a single-exponential function and were subsequently truncated to ~6 half-lives based on the estimated rate constant. Trajectories longer than 10 s were decimated to 0.5 Hz. The dependence of binding or kinetics on ClpP concentration, ATP concentration, or ADEP-2B concentration was fitted to appropriate equations using Prism or KaleidaGraph.

ACKNOWLEDGEMENTS

We thank D. Carney for synthesis of ADEP-2B and B. Hall, A. Martin, A. Olivares, D. Pheasant, B. Stein, B. Stinson, and O. Yosefson for assistance and advice. Supported by N.I.H. grants GM-101988 and S10 OD016326. BLI experiments were performed in the M.I.T. Biophysical Instrument Facility. T.A.B. is an employee of the Howard Hughes Medical Institute. K.R.S. was supported by a Charles A. King Trust Postdoctoral Research Fellowship, Bank of America, N.A., Co-Trustee.

References

(1). Baker TA, Sauer RT. ClpXP, an ATP-powered unfolding and proteindegradation machine. Biochim. Biophys. Acta. 2012; 1823:15–28. [PubMed: 21736903]

(2). Grimaud R, Kessel M, Beuron F, Steven AC, Maurizi MR. Enzymatic and structural similarities between the Escherichia coli ATP-dependent proteases, ClpXP and ClpAP. J. Biol. Chem. 1998; 273:12476–12481. [PubMed: 9575205]

(3). Jones JM, Welty DJ, Nakai H. Versatile action of *Escherichia coli* ClpXP as protease or molecular chaperone for bacteriophage Mu transposition. J. Biol. Chem. 1988; 273:459–465.

(4). Burton RE, Baker TA, Sauer RT. Energy-dependent degradation: Linkage between ClpXP-catalyzed nucleotide hydrolysis and protein-substrate processing. Protein Sci. 2003; 12:893–902. [PubMed: 12717012]

(5). Joshi SA, Hersch GL, Baker TA, Sauer RT. Communication between ClpX and ClpP during substrate processing and degradation. Nat. Struct. Mol. Biol. 2004; 11:404–411. [PubMed: 15064753]

(6). Martin A, Baker TA, Sauer RT. Rebuilt AAA+ motors reveal operating principles for ATP-fueled machines. Nature. 2005; 437:1115–120. [PubMed: 16237435]

(7). Stinson BM, Nager AR, Glynn SE, Schmitz KR, Baker TA, Sauer RT. Nucleotide binding and conformational switching in the hexameric ring of a AAA+ machine. Cell. 2013; 153:628–639. [PubMed: 23622246]

(8). Stinson BM, Baytshtok V, Schmitz KR, Baker TA, Sauer RT. Subunit asymmetry and roles of conformational switching in the hexameric AAA+ ring of ClpX. Nat. Struct. Mol. Biol. 2015; 22:411–416. [PubMed: 25866879]

(9). Iosefson O, Nager AR, Baker TA, Sauer RT. Coordinated gripping of substrate by subunits of a AAA+ proteolytic machine. Nat. Chem. Biol. 2015a; 11:201–206. [PubMed: 25599533]

(10). Aubin-Tam ME, Olivares AO, Sauer RT, Baker TA, Lang MJ. Single-molecule protein unfolding and translocation by an ATP-fueled proteolytic machine. Cell. 2011; 145:257–267. [PubMed: 21496645]

(11). Maillard RA, Chistol G, Sen M, Righini M, Tan J, Kaiser CM, Hodges C, Martin A, Bustamante C. ClpX(P) generates mechanical force to unfold and translocate its protein substrates. Cell. 2011; 145:459–469. [PubMed: 21529717]

(12). Sen M, Maillard RA, Nyquist K, Rodriguez-Aliaga P, Pressé S, Martin A, Bustamante C. The ClpXP protease unfolds substrates using a constant rate of pulling but different gears. Cell. 2013; 155:636–646. [PubMed: 24243020]

(13). Cordova JC, Olivares AO, Shin Y, Stinson BM, Calmat S, Schmitz KR, Aubin-Tam M-E, Baker TA, Lang MJ, Sauer RT. Stochastic but highly coordinated protein unfolding and translocation by the ClpXP proteolytic machine. Cell. 2014; 158:647–658. [PubMed: 25083874]

(14). Olivares AO, Nager AR, Yosefson O, Sauer RT, Baker TA. Mechanochemical basis of protein degradation by a double-ring AAA+ machine. Nat. Struct. Mol. Biol. 2014; 21:871–875. [PubMed: 25195048]

(15). Iosefson O, Olivares AO, Baker TA, Sauer RT. Dissection of axial-pore loop function during unfolding and translocation by a AAA+ proteolytic machine. Cell Rep. 2015b; 12:1032–1041. [PubMed: 26235618]

(16). Martin A, Baker TA, Sauer RT. Distinct static and dynamic interactions control ATPase-peptidase communication in a AAA+ protease. Mol. Cell. 2007; 27:41–52. [PubMed: 17612489]

(17). Kim YI, Levchenko I, Fraczkowska K, Woodruff RV, Sauer RT, Baker TA. Molecular Determinants of Complex Formation between Clp/Hsp100 ATPases and the ClpP Peptidase. Nat. Struct. Biol. 2001; 8:230–233. [PubMed: 11224567]

(18). Singh SK, Rozycki J, Ortega J, Ishikawa T, Lo J, Steven AC, Maurizi MR. Functional domains of the ClpA and ClpX molecular chaperones identified by limited proteolysis and deletion analysis. J. Biol. Chem. 2001; 276:29420–29429. [PubMed: 11346657]

(19). Lee BG, Park EY, Lee KE, Jeon H, Sung KH, Paulsen H, Rübsamen-Schaeff H, Brötz-Oesterhelt H, Song HK. Structures of ClpP in complex with acyldepsipeptide antibiotics reveal its activation mechanism. Nat. Struct. Mol. Biol. 2010; 17:471–478. [PubMed: 20305655]

(20). Li DH, Chung YS, Gloyd M, Joseph E, Ghirlando R, Wright GD, Cheng YQ, Maurizi MR, Guarné A, Ortega J. Acyldepsipeptide antibiotics induce the formation of a structured axial channel in ClpP: A model for the ClpX/ClpA-bound state of ClpP. Chem. Biol. 2010; 17:959–969. [PubMed: 20851345]

(21). Schmitz KR, Carney DW, Sello JK, Sauer RT. The crystal structure of *M. tuberculosis* ClpP1P2 suggests a model for peptidase activation by AAA+ partner binding and substrate delivery. Proc. Natl. Acad. Sci. USA. 2014; 111:E4587–4595. [PubMed: 25267638]

(22). Brötz-Oesterhelt H, Beyer D, Kroll H-P, Endermann R, Ladel C, Schroeder W, Schroeder W, Hinzen B, Raddatz S, Paulsen H, Henninger K, Bandow JE, Sahl HG, Labischinski H.

Dysregulation of bacterial proteolytic machinery by a new class of antibiotics. Nat. Med. 2005; 11:1082–1087. [PubMed: 16200071]

(23). Kirstein J, Hoffmann A, Lilie H, Schmidt R, Rübsamen-Waigmann H, Brötz-Oesterhelt H, Mogk A, Turgay K. The antibiotic ADEP reprogrammes ClpP, switching it from a regulated to an uncontrolled protease. EMBO Mol. Med. 2009; 1:37–49. [PubMed: 20049702]

(24). Abdiche Y, Malashock D, Pinkerton A, Pons J. Determining kinetics and affinities of protein interactions using a parallel real-time label-free biosensor, the Octet. Anal. Biochem. 2008; 377:209–217. [PubMed: 18405656]

(25). Shin Y, Davis JH, Brau RR, Martin A, Kenniston JA, Baker TA, Sauer RT, Lang MJ. Single-molecule denaturation and degradation of proteins by the AAA+ ClpXP protease. Proc. Natl. Acad. Sci. USA. 2009; 106:19340–19345. [PubMed: 19892734]

(26). Glynn SE, Nager AR, Baker TA, Sauer RT. Dynamic and static components power unfolding in topologically closed rings of a AAA+ proteolytic machine. Nat. Struct. Mol. Biol. 2012; 19:616–622. [PubMed: 22562135]

(27). Lee ME, Baker TA, Sauer RT. Control of substrate gating and translocation into ClpP by channel residues and ClpX binding. J. Mol. Biol. 2010; 399:707–718. [PubMed: 20416323]

(28). Carney D, Schmitz KR, Truong J, Sauer RT, Sello JK. Restriction of the conformational dynamics of the cyclic acyldepsipeptide macrocycle improves antibacterial activity by enhancing both ClpP peptidase binding and activation. J. Amer. Chem. Soc. 2014; 136:1922–1929. [PubMed: 24422534]

(29). Glynn SE, Martin A, Nager AR, Baker TA, Sauer RT. Crystal structures of asymmetric ClpX hexamers reveal nucleotide-dependent motions in a AAA+ protein-unfolding machine. Cell. 2009; 139:744–756. [PubMed: 19914167]

(30). Hersch GL, Burton RE, Bolon DN, Baker TA, Sauer RT. Asymmetric interactions of ATP with the AAA+ $ClpX_6$ unfoldase: allosteric control of a protein machine. Cell. 2005; 121:1017–1027. [PubMed: 15989952]

(31). Nager AR, Baker TA, Sauer RT. Stepwise unfolding of a β-barrel protein by the AAA+ ClpXP protease. J. Mol. Biol. 2011; 413:4–16. [PubMed: 21821046]

(32). Kenniston JA, Baker TA, Fernandez JM, Sauer RT. Linkage between ATP consumption and mechanical unfolding during the protein processing reactions of an AAA+ degradation machine. Cell. 2003; 114:511–520. [PubMed: 12941278]

(33). Too PH, Erales J, Simen JD, Marjanovic A, Coffino P. Slippery substrates impair function of a bacterial protease ATPase by unbalancing translocation versus exit. J. Biol. Chem. 2013; 288:13243–13257. [PubMed: 23530043]

(34). Vass RH, Chien P. Critical clamp loader processing by an essential AAA+ protease in *Caulobacter crescentus*. Proc. Natl. Acad. Sci. USA. 2013; 110:18138–18143. [PubMed: 24145408]

(35). Sauer RT, Baker TA. AAA+ proteases: ATP-fueled machines of destruction. Ann. Rev. Biochem. 2011; 80:587–612. [PubMed: 21469952]

(36). Park S, Li X, Kim HM, Singh CR, Tian G, Hoyt MA, Lovell S, Battaile KP, Zolkiewski M, Coffino P, Roelofs J, Cheng Y, Finley D. Reconfiguration of the proteasome during chaperone-mediated assembly. Nature. 2013; 497:512–516. [PubMed: 23644457]

(37). Beckett D, Kovaleva E, Schatz PJ. A minimal peptide substrate in biotin holoenzyme synthetase-catalyzed biotinylation. Protein Sci. 1999; 8:921–929. [PubMed: 10211839]

(38). Nørby J. Coupled assay of Na+,K+-ATPase activity. Methods Enz. 1988; 156:116–119.

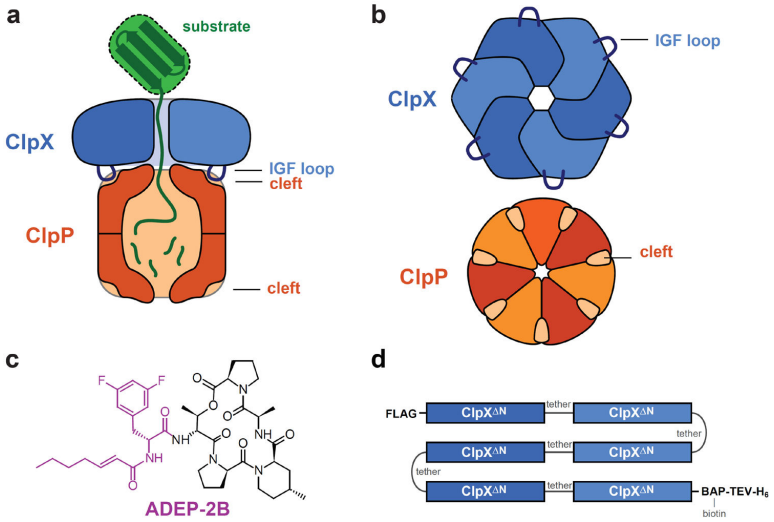

Figure 1.

The ClpXP protease. **a**) Side view of ClpXP degrading a substrate (green). A ClpX hexamer (blue) recognizes, unfolds, and translocates protein substrates into the degradation chamber of ClpP (dark orange), which consists of two heptameric rings. ClpXP is principally stabilized by interactions between the IGF loops of ClpX and hydrophobic clefts on each ClpP ring. **b**) Axial view of a ClpX homohexameric ring and a ClpP homoheptameric ring, highlighting the interaction elements. **c**) Chemical structure of ADEP-2B.[21,28] The portion thought to mimic binding of an IGF tripeptide is colored purple. **d**) $^{sc6}ClpX^{\Delta N}$-bio is a single-chain pseudohexamer in which the $ClpX^{\Delta N}$ subunits are linked by six-residue tethers. The protein contains an N-terminal FLAG tag and a C-terminal sequence consisting of a biotin acceptor peptide (BAP), a cleavage site for Tobacco Etch Virus protease (TEV), and six histidines (H_6).

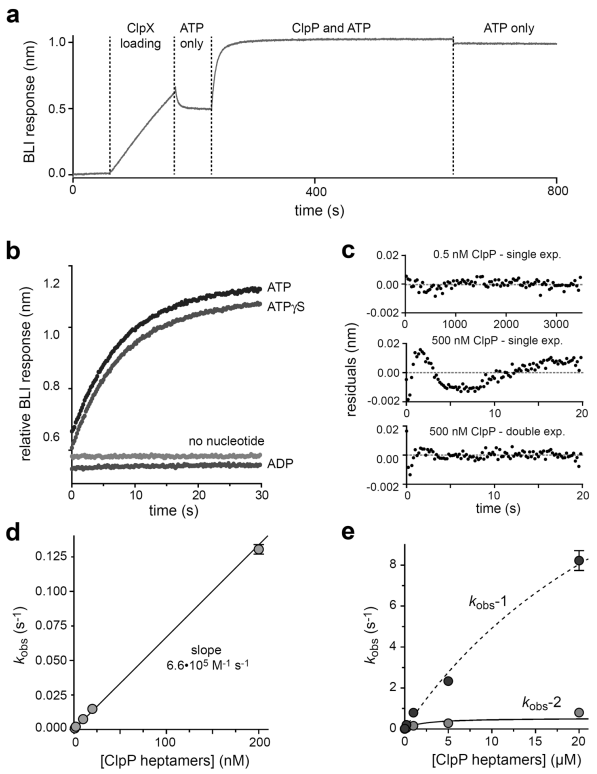

Figure 2.

Association of ClpP with $^{sc6}ClpX^{\Delta N}$-bio assayed by BLI. **a**) A streptavidin-coated BLI biosensor was incubated sequentially with buffer, buffer plus 20 nM $^{sc6}ClpX^{\Delta N}$-bio, buffer plus 2 mM ATP, buffer plus 200 nM ClpP and 2 mM ATP, and buffer plus 2 mM ATP. **b**) BLI trajectories showing that ClpP binding to $^{sc6}ClpX^{\Delta N}$-bio occurs with similar kinetics in the presence of ATP or ATP**γ**S (2 mM each). Binding was not observed with 2 mM ADP or no nucleotide. Individual trajectories are offset to allow comparisons. **c**) Residuals of single-exponential and/or double-exponential fits for association trajectories obtained using ClpP concentrations of 0.5 or 500 nM. **d**) For ClpP concentrations of 200 nM or less, rate constants from single-exponential fits of ClpP association trajectories (k_{obs}) varied linearly with ClpP, with a slope corresponding to the second-order association rate constant. **e**) Variation of the rate constants from double-exponential fits for ClpP concentrations of 500 nM or higher. The curves are fits to a hyperbolic equation. For k_{obs}-1 (amplitude ~70%), the maximal rate was 22 ± 7 s^{-1} with a half-maximal concentration of ~35 μM ClpP heptamer. For k_{obs}-2 (amplitude ~30%), the maximal rate was 0.54 ± 0.2 s^{-1} with a half-maximal concentration of ~2 μM ClpP heptamer.

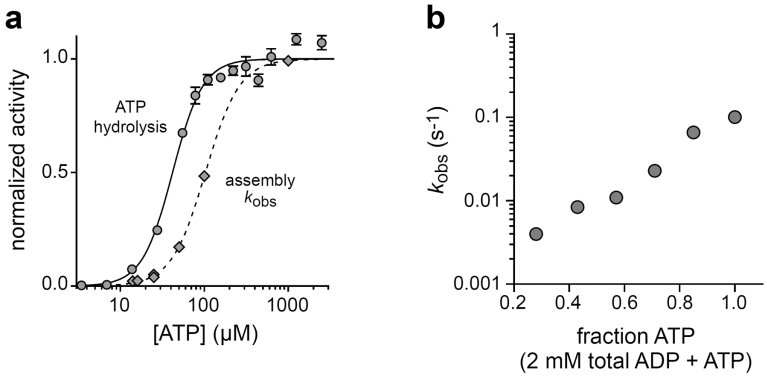

Figure 3.

Nucleotide dependence of ClpP association. **a**) Graphs showing normalized ^{sc6}ClpX$^{\Delta N}$-bio ATP-hydrolysis activity and normalized ClpP association rate constants (obtained using 200 nM ClpP) as a function of ATP concentration. The curves are fits to a Hill equation ($Y = [ATP]^n/(K_{app}{}^n + [ATP]^n)$). For ATP hydrolysis, the fitted values of K_{app} and n were 42 ± 3 μM and 2.4 ± 0.3, respectively. For assembly, these fitted values were 100 ± 2 μM and 2.1 ± 0.06, respectively. Maximal fitted values prior to normalization were 73 ± 1 min^{-1} enz^{-1} for ATP hydrolysis and 0.138 ± 0.001 s^{-1} for k_{obs}. **b**) Variation of k_{obs} for 200 nM ClpP association with the fraction of ATP in mixtures with ADP (2 mM total nucleotide).

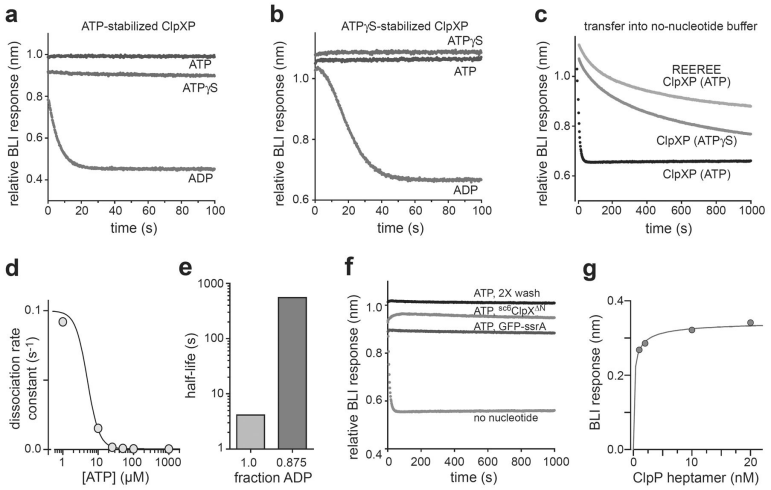

Figure 4.

Dissociation and equilibrium stability of ClpXP complexes. **a**) Complexes were assembled with ^{sc6}ClpX$^{\Delta N}$-bio bound to the biosensor, 200 nM ClpP, and 2 mM ATP. At time zero, the biosensor was moved into ClpP-free buffer containing 2 mM ADP, 2 mM ATP, or 2 mM ATPγS. The trajectories have been offset vertically, but all start at the same BLI value ± 5%. **b**) The same experiment as shown in panel A, except ClpXP complexes were assembled in the presence of 2 mM ATPγS. **c**) Dissociation kinetics after transfer into buffer without nucleotide for ClpP complexes assembled with ATPase-active ^{sc6}ClpX$^{\Delta N}$-bio and ATP (bottom curve), ATPase-active ^{sc6}ClpX$^{\Delta N}$-bio and ATPγS (middle curve) or a ATP-hydrolysis defective REEREE ^{sc6}ClpX$^{\Delta N}$-bio variant and ATP (top curve). **d**) Complexes were assembled with ATP as in panel **a** and then transferred into ClpP-free buffer containing different concentrations of ATP. Dissociation rate constants were calculated from single-exponential fits and plotted as a function of the ATP concentration. The line is a fit to the Hill equation. **e**) Half-lives of ClpXP complexes assembled in ATP following transfer into buffer containing 100% ADP (2 mM) or 87.5% ADP (1.75 mM ADP; 0.25 mM ATP). (**f**) BLI trajectories showing that ClpXP complexes are stable for long periods in ClpP-free buffer containing 2 mM ATP, 2 mM ATP and unbiotinylated ^{sc6}ClpX$^{\Delta N}$ (1 μM), or 2 mM ATP and GFP-ssrA (20 μM). **g**) Equilibrium BLI response for ^{sc6}ClpX$^{\Delta N}$-bio binding as a function of total ClpP concentration. The fitted curve is a hyperbolic equation with half-maximal binding at a total ClpP concentration of 160 ± 75 pM.

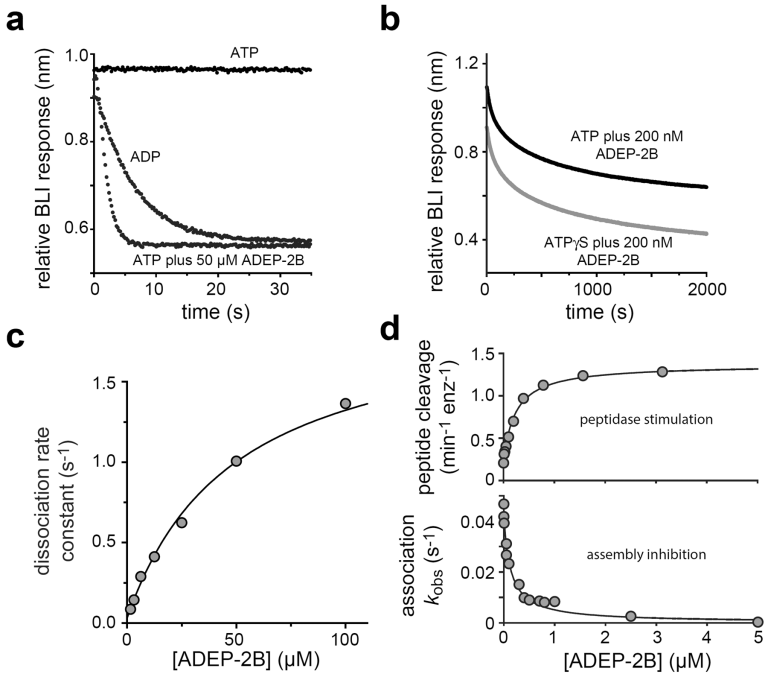

Figure 5.

ADEP effects. **a**) BLI trajectories following transfer of ATP-stabilized ClpXP into ClpP-free buffer containing 2 mM ATP without or with 50 μM ADEP-2B. **b**) BLI trajectories following transfer of ATP-stabilized ClpXP into ClpP-free buffer containing 200 nM ADEP-2B and 2 mM ATP or ATPγS. **c**) ADEP-2B stimulation of dissociation. ATP-stabilized ClpXP was transferred into ClpP-free buffer containing 2 mM ATP and different ADEP-2B concentrations, and dissociation rate constants were determined by single-exponential fits. The line is a hyperbolic fit (R^2 = 0.994) with values of 2.0 ± 0.13 s^{-1} for the maximum rate and 50 ± 7 μM for half-maximal stimulation. Sigmoidal equations for mechanisms involving two ADEPs ($\alpha^2/(1+2\alpha+\alpha^2)$; α = [ADEP]/K_μ; R^2 = 0.971) or three ADEPs ($\alpha^3/(1+3\alpha+3\alpha^2+\alpha^3)$; R^2 = 0.958) gave poorer fits. **d**) (top) ADEP-2B stimulation of decapeptide cleavage of 25 nM ClpP. The line is a hyperbolic fit (R^2 = 0.995) with half-maximal inhibition at a total concentration of 240 ± 26 nM. (bottom) ADEP-2B inhibition of association of 200 nM ClpP. The line is a hyperbolic fit (R^2 = 0.981) with half-maximal inhibition at a total concentration of 167 ± 20 nM.

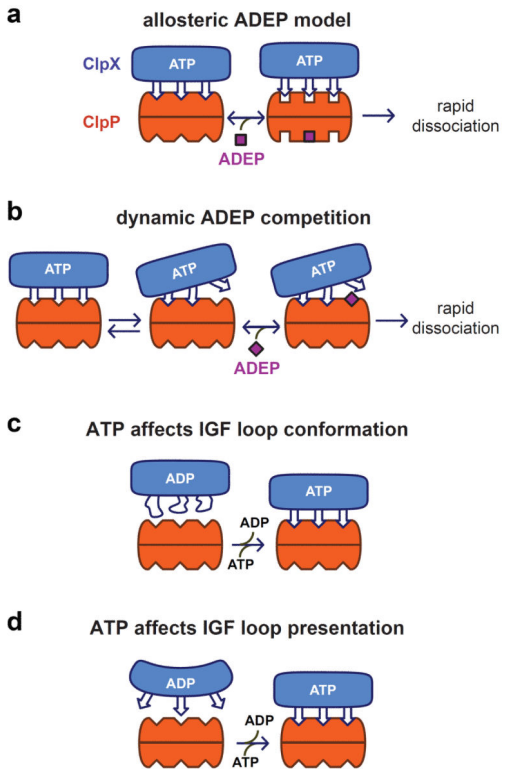

Figure 6.

Models for small-molecule control of complex stability. **a**) ADEP binding to an empty ClpP cleft allosterically stabilizes a conformation from which ClpX rapidly dissociates. For simplicity, only a subset of IGF loops in ClpX and clefts in each ring of ClpP are shown. **b**) ADEP binding to a ClpP cleft transiently unoccupied by an IGF loop prevents re-docking and stimulates dissociation. **c**) ATP binding to the ClpX hexamer stabilizes a conformation of the IGF loops that binds the ClpP clefts more efficiently. **d**) ATP binding to the ClpX hexamer positions the IGF loops to interact optimally with ClpP.